IEEE Access
Multidisciplinary ⋮ Rapid Review ⋮ Open Access Journal

Received 16 November 2023, accepted 8 January 2024, date of publication 19 January 2024, date of current version 29 January 2024.

Digital Object Identifier 10.1109/ACCESS.2024.3355950

RESEARCH ARTICLE

Comparative Studies on Performances of Slotted and Slotless High-Speed PMBLDC Motors

JING ZHAO[1], (Member, IEEE), WEI HE[1], WENQI FU[2], YU DING[1], AND YOUGUANG GUO[3], (Senior Member, IEEE)

[1]School of Automation, Beijing Institute of Technology, Beijing 100081, China
[2]Beijing Institute of Aerospace Control Devices, Beijing 100039, China
[3]School of Electrical and Data Engineering, University of Technology Sydney, Sydney, NSW 2007, Australia

Corresponding author: Wei He (hewei066@163.com)

This work was supported in part by the National Natural Science Foundation of China under Grant 51977011, and in part by the Beijing Key Laboratory of Long-Life Technology of Precise Rotation and Transmission Mechanisms under Project BZ0388202202.

ABSTRACT Slotted and slotless stators are two main stator topologies in high-speed permanent magnet brushless direct current (PMBLDC) motors. Both have their own advantages and drawbacks. The electromagnetic loss of slotted and slotless motors have different characteristics in different speed range. Therefore, the comparison of slotted and slotless motors must consider different speed ranges. The performances of slotted and slotless high-speed PMBLDC motors in the full speed range up to 480 krpm are compared in this paper. The no-load and load electromagnetic performances of slotted and slotless motors are studied. The electromagnetic losses of slotted and slotless motors in the full speed range are investigated and compared. Meanwhile, based on the loss calculation results, the thermal characteristics of slotted and slotless motors are studied. The comparison results are summarized considering the electromagnetic, loss and thermal characteristics comprehensively. Finally, a prototype of high-speed PMBLDC motor is manufactured and tested to validate the analysis results.

INDEX TERMS High speed, permanent magnet brushless DC (PMBLDC) motor, slotted, slotless, comparison, electromagnetic performance, losses, temperature rise.

I. INTRODUCTION

With the development of industry and advanced science and technology, the motor speed is increasing. The high-speed motor is directly connected with the high-speed prime mover or load, which eliminates the intermediate transmission parts and greatly improves the transmission efficiency. The high-speed motor has broad application prospects in turbine, air compressor, high-speed pump, flywheel energy storage and other applications [1], [2]. High-speed motor structure has various motor types [3], [4], [5], among which permanent magnet brushless direct current (PMBLDC) motor has become a research hotspot due to its advantages of high efficiency and power density. Sometimes the rotor speed of PMBLDC motor can reach hundreds of thousands of revolutions per minute, and the high-speed PM motors present more prominent problems in electromagnetic design, losses, temperature rise and other aspects, which have received more and more attentions.

Stator structures of high-speed PMBLDC motors commonly include slotted structure [6] and slotless structure [7]. The stator windings of slotted motor are embedded in the stator slots. Compared with slotted motors, slotless motors eliminate the stator teeth and only retain the stator back iron.

The slotted stator structure is beneficial to protect the windings from the influence of air-gap magnetic field space harmonics. Although the slotted high-speed PMBLDC motor has high power density, its loss density is normally high. Thus the losses and thermal problems have attracted more and more attentions. Reference [6] proposed a thermal analysis model for a 60 krpm slotted high-speed PM motor considering the multiple physical fields coupling. Considering that the iron loss of slotted PM motor is usually high and has a great influence on motor performance, amorphous alloy material or soft

The associate editor coordinating the review of this manuscript and approving it for publication was Zhuang Xu.

magnetic composite (SMC) material can be used to reduce the stator high frequency iron loss [8], [9]. Reference [10] discussed the influence of speed on the losses of slotted high-speed PM motor, but the maximum speed researched is 15 krpm, without considering higher speed range. These literatures only studied the slotted high-speed motors and did not carry out the comparison with the slotless motors.

In order to eliminate the cogging torque, and reduce the stator iron loss and the rotor loss produced by harmonic magnetic field caused by slotting in slotted PM motors, slotless PM motors have attracted more and more attention [7], [11], [12], [13]. Reference [11] proposed a slotless motor with a maximum speed of 300 krpm, and presented the variation rule of the no-load losses with the speed under different working conditions, but did not classify the no-load losses in detail. Reference [12] studied a slotless high-speed PM motor with a maximum speed of 150 krpm, and measured copper loss, windage loss, stator and rotor iron losses of the motor within the entire speed range. In [13], an analytical model of eddy current and eddy current loss of a slotless PM motor was established and validated by finite element method (FEM).

Compared with slotless PM motor, the slotted PM motor has a smaller equivalent air gap because its teeth are located inside the stator winding, which usually results in higher air gap flux density, and also has spatial harmonics and larger armature reaction and the cogging torque [14]. The slotted and slotless high-speed PM motors have their respective advantages and characteristics. Reference [14] compared the torque capability of slotted and slotless PM motors. Reference [15] pointed out that compared with slotless BLDC motor, the slotted BLDC motor has greater power and torque fluctuation. Reference [16] compared the torque characteristics of slotted and slotless PM motors by using analytical method. Reference [17] mainly compared the power density of the two kinds of motors. References [14], [15], [16], and [17] mainly compared the torque and power performances of slotted and slotless PM motors, without considering electromagnetic losses.

There are a few comparative studies on the losses and thermal characteristics between slotted and slotless PM motors. In [18], the distributions of electromagnetic losses at nominal working condition of slotted and slotless PM motors were compared. Reference [19] compared the electromagnetic and losses performances of slotted and slotless PM motors with toroidal windings. Reference [20] compared the electromagnetic and loss properties of slotted and slotless PM motors with 4 different PM magnetizations. However, in [18], [19], and [20], the effect of speed was not taken into account. Different speed ranges may lead to different comparison results, thus affecting the accuracy of comparison conclusions. Moreover, the temperature field was not considered.

To sum up, the comprehensive comparation on the electromagnetic losses within the full speed range between the slotted and slotless PM motors is very important. Generally, the slotted motors have higher iron losses, while the slotless motors have higher winding losses. However, the changing degrees of different losses with speed are not exactly the same, which may influence the stator topology selection of high speed PM motors. Moreover, there are some differences in the electromagnetic and temperature rise characteristics between slotted and slotless PM motors. Therefore, it is necessary to conduct in-depth comparative study on electromagnetic performance, losses and temperature rise of slotted and slotless high-speed PMBLDC motors.

In this paper, slotted and slotless high-speed PMBLDC motors are designed to adapt to high speed conditions up to 480 krpm firstly. Then the no-load and load electromagnetic performances are compared. The stator and rotor losses of slotted and slotless motors in the full speed range of 0-480 krpm are comparatively analyzed. In addition, the temperature rise characteristics of slotted and slotless high-speed PMBLDC motors are studied based on the loss calculation results. Finally, the analysis results are validated by the measurements on a prototype of high-speed PMBLDC motor.

TABLE 1. Basic parameters of PMBLDC motors.

Parameter	Value	Unit
Rated torque T_N	50	mNm
Rated current density J_N	6.48	A/mm^2
Stator outer diameter D_{so}	55	mm
Rotor outer diameter D_{ro}	26(Slotted)/29.2(Slotless)	mm
Rotor inner diameter D_{ri}	9	mm
Axial length l_{ef}	18	mm
Thickness of PM l_{pm}	2(Slotted)/3.6(Slotless)	mm
Thickness of retaining sleeve l_{rs}	2	mm
PM material	N38SH	

II. ELECTROMAGNETIC DESIGN AND ANALYSIS OF HIGH-SPEED PMBLDC MOTORS

Considering high-speed working conditions, the slotted and slotless high-speed PMBLDC motor compared in this paper adopt internal rotor structure with surfaced PMs and stainless steel retaining sleeve for PMs, and the pole-slot combination is 2 poles and 12 slots, as shown in Fig. 1. In order to improve the sinusoidal degree of the back electromotive force, the motor adopts distributed winding with a pitch of 5. Larger equivalent air gap length of the slotless PMBLDC motor results in smaller magnetic flux than the slotted motor. Thus, the PM outer diameter and volume of slotless PMBLDC motor are appropriately increased to ensure that the amplitude of no-load back EMF of the slotless motor is almost the same as that of the slotted motor, which is the basis for the comparative research. The thickness of retaining sleeve of slotted and slotless motor is set to 2 mm to offset the huge centrifugal force generated by high speed operation of the rotor. The thickness of the rotor core of both motors is the same. The structure parameters of slotted and slotless motors are optimized to ensure the superiority of motor performance. The main parameters of slotted and slotless motors are shown in Table 1.

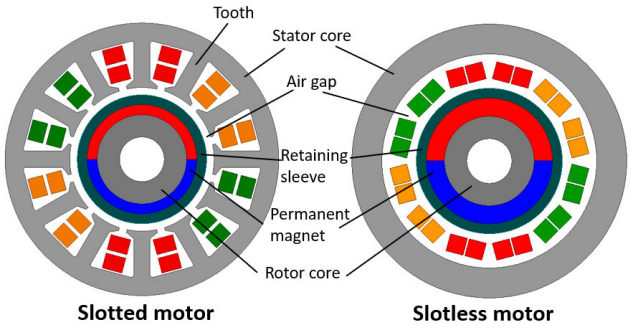

FIGURE 1. Diagram of slotted and slotless high-speed PMBLDC motors.

A. NO-LOAD ELECTROMAGNETIC CHARACTERISTICS

The magnetic field distributions and radial air-gap flux density at no-load of slotted and slotless high-speed PMBLDC motors are compared in Figs. 2 and 3. As seen from Fig. 2, the magnetic force line of the slotted motor links with the winding through the stator teeth, and there is only a small amount of magnetic leakage at the tooth tip position, which shows a high utilization of PMs. Compared with the slotted motor, the magnetic field distribution of the slotless motor is more uniform and unsaturated. As seen from Fig. 3(a), the amplitude of radial air-gap flux density of both motors is basically the same although their equivalent air gap length is different. This is obtained by increasing the outer diameter and volume of PM of slotless motor. It can be seen from Fig.3(b) that the harmonic contents of slotted motor are a little higher, mainly the 11th and 13th harmonics due to the slotting effect, while the slotless motor has almost no higher order harmonics.

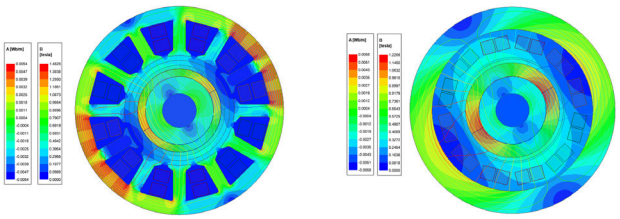

FIGURE 2. Comparison of magnetic flux density distributions of the two motors: (a) slotted motor, and (b) slotless motor.

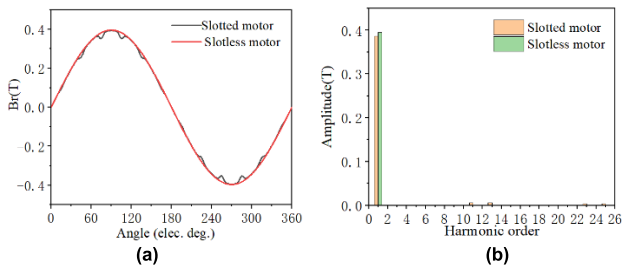

FIGURE 3. Comparison of air-gap radial magnetic flux density: (a) waveforms, and (b) harmonics.

Because of stator slotting, the air gap reluctance distribution of slotted motor is not uniform, resulting in cogging torque with a peak-to-peak value of 0.055 mNm, as shown in Fig. 4. The slotless motor has eliminated the stator tooth structure, so the air gap reluctivity is evenly distributed, and the cogging torque is almost zero, which is not shown. No-load back EMF is another important index to evaluate the no-load performance of motor. As shown in Fig. 5, the no-load back EMF waveforms of both slotted and slotless motors are sine waves, and the waveforms basically coincide with each other.

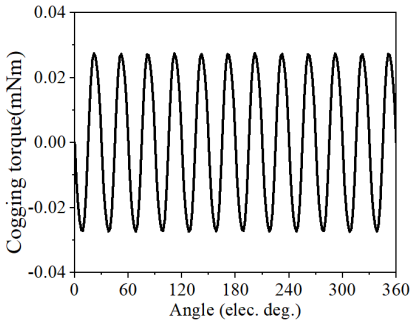

FIGURE 4. Cogging torque of slotted motor.

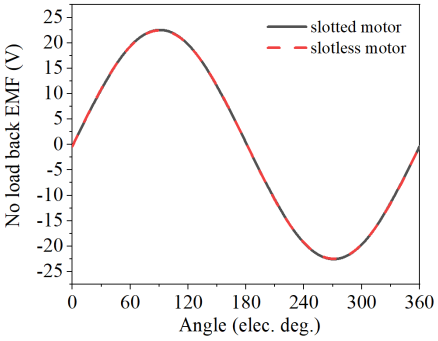

FIGURE 5. No load back EMF.

B. ELECTROMAGNETIC CHARACTERISTICS UNDER LOAD CONDITION

The rated currents of slotted and slotless motors are basically the same, but the overload characteristics are different. The average torques and torque ripples of the two motors at different loads are compared in Fig. 6. It can be seen from Fig. 6 that: 1) For the slotted motor, when the input current increases from rated current to 9 times overload, the corresponding average torque is increasing with the corresponding current, but the torque coefficient is decreased at high overload, which is caused by the saturation as shown in Fig. 2(a); 2) For the slotless motor, the corresponding average torque has a linear relationship with the overload degree, indicating that the overload capacity of the slotless motor is better than that of the slotted motor, which is caused by the larger equivalent air gap; 3) Whether under rated load or overload condition, the torque fluctuation of slotless motor is lower than that of slotted motor, which is related to the fact that the slotless

motor basically eliminates the space harmonics of air gap magnetic field.

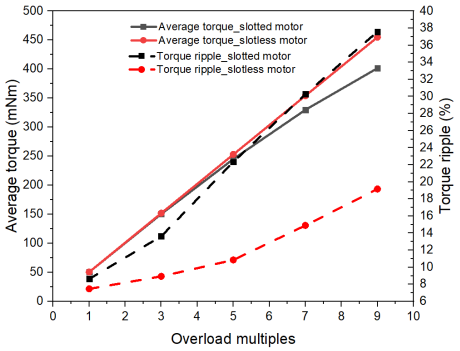

FIGURE 6. Comparison of average torque and torque ripple of slotted and slotless motors at different loads.

III. ELECTROMAGNETIC LOSS ANALYSIS

Due to the characteristics of high-speed and high frequency, it is necessary to pay attention to the losses of the high-speed PMBLDC motor. The main losses of high-speed PMBLDC motor include stator losses and rotor losses. The stator losses can be subdivided into iron loss and winding loss, and the rotor loss is mainly the rotor eddy current loss. This section studies the losses characteristics of the slotted and slotless high-speed PMBLDC motors.

A. STATOR IRON LOSSES

When the PMBLDC motor runs at high speed, the alternating frequency of magnetic field is very high, and hence the stator iron loss is large. As the frequency is positively correlated with the speed, the speed has a great influence on the stator iron losses. Moreover, the thickness of silicon steel sheet also has a great influence on the iron losses. However, the costs of different thickness of silicon steel material normally vary greatly. Considering different requirements, two grades of silicon steel sheet of iron core are chosen to be compared: one is the 35SW1900 with sheet thickness of 0.35 mm and much lower price, and the other is the 20SW1500 with sheet thickness of 0.2 mm. The BH and BP curves of both materials are shown in Fig. 7. The BP curves are at the frequency of 1000 Hz. It is shown that the BH curves of both materials are basically coincident but the loss of 35SW1900 is much larger than that of 20SW1500 with the same magnetic flux density B.

In order to accurately calculate the iron losses, the BP curves at different frequencies are input into the finite element software. The maximum frequency of 35SW1900 is 8000 Hz, and the maximum frequency of 20SW1500 reaches 10000 Hz, all meeting or exceeding the 8000 Hz at 480 krpm. Fig. 8 shows the change of stator iron losses with speed and different silicon steel materials. It can be seen that: 1) The stator iron losses increase in a parabolic nonlinear manner with the increasing of speed. 2) The stator iron loss of slotless motor is lower than that of slotted motor

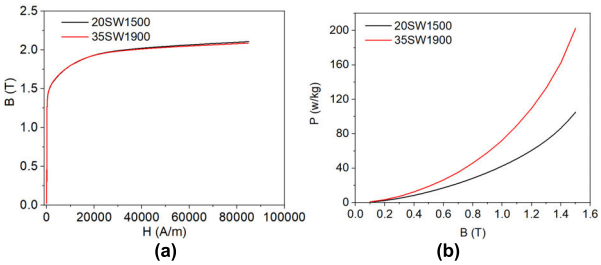

FIGURE 7. Comparison of BH and BP curves: (a) BH curve, and (b) BP curve.

at the same speed, and the difference increases with speed increasing. 3) For both slotted and slotless motors, the iron loss at load is larger than that at no load. However, for slotted motor, the difference is great, while for slotless motor, the difference is not obvious. It is believed that this phenomenon is related to armature reaction. In slotted motor, the armature reaction is large, and stator magnetomotive force has great influence on stator magnetic field. In slotless motor, the armature reaction is small, and stator magnetomotive force has little influence on stator magnetic field. 4) The stator iron losses with 20SW1500 is much smaller than that with 35SW1900. Therefore, 20SW1500 is selected as the material of stator and rotor cores in the following study of winding losses and rotor losses.

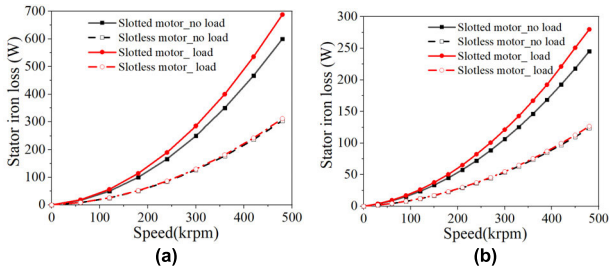

FIGURE 8. Comparison of stator iron losses of slotted and slotless motors versus different speed with different silicon steel materials: (a) 35SW1900, and (b) 20SW1500.

B. WINDING LOSSES

For high-speed PMBLDC motor with high frequency, the current may not be uniformly distributed in the conductor due to the skin effect and proximity effect, which make the effective conductive area of the circular wire smaller and the equivalent resistance increases. The increased part of the resistance based on the DC resistance is the so-called AC resistance. In a round bunch of N round conductors, the ratio of AC resistance R_{ac} to DC resistance R_{dc} can be used to calculate the influence of skin effect and proximity effect on the winding loss, and its expression is as follows [21]:

$$\frac{R_{ac}}{R_{dc}} = 1 + \frac{1}{48}\left(\frac{a}{\delta_x}\right)^4 + \frac{\xi N}{8\pi}\left(\frac{a}{\delta_x}\right)^4$$

TABLE 2. AC/DC resistance ratio at different diameter and frequency.

Dia.(mm) / Fre. (Hz)	0.3	0.7	1.1	1.5	1.9	2.3
1000	1.0000	1.0002	1.0014	1.0047	1.0121	1.0260
2000	1.0000	1.0009	1.0054	1.0188	1.0485	1.1041
3000	1.0001	1.0020	1.0123	1.0424	1.1091	1.2342
4000	1.0001	1.0036	1.0218	1.0753	1.1939	1.4164
5000	1.0002	1.0056	1.0340	1.1177	1.3030	1.6506
6000	1.0003	1.0080	1.0490	1.1695	1.4363	1.9369
7000	1.0004	1.0109	1.0667	1.2307	1.5939	2.2752
8000	1.0005	1.0143	1.0871	1.3013	1.7756	2.6656

$$= 1 + (k_s + k_p)\left(\frac{a}{\delta_x}\right)^4 \tag{1}$$

where a is the radius of the circular wire, δ_x is the classical skin depth, $\xi = \frac{Nd^2}{4R^2}$, d is the diameter of the circular wire, R is the radius of circular bunch, k_s is the skin effect coefficient, and k_p is the proximity effect coefficient.

When $N = 12$ and all conductors are connected in series, and all the round conductors are arranged relatively closely in a round bunch, $\xi = 0.551$, $k_s = 0.0208$, $k_p = 0.263$, $k_p = 12.644k_s$, which means the influence of proximity effect on winding AC loss is much greater than that of skin effect. The change of AC/ DC resistance ratio R_{ac}/R_{dc} with different wire diameter and frequency is shown in Table 2. As seen from the table, with the increases of frequency and wire diameter, the AC/DC resistance ratios increase, indicating that the skin effect and proximity effect cannot be ignored in this study. Thus, the conductor AC loss p_{ac} can be directly calculated by the Joule heat formula as follows:

$$P_{ac} = mI_{rms}^2 R_{ac} \tag{2}$$

where m is the number of motor phases, and I_{rms} is the root-mean-square (RMS) current.

In addition, due to the difference among flux linkages of parallel conductors in a stator winding, the winding circulating current loss can be caused. In this paper, the conductor transposition or twist is adopted to reduce the circulation loss to a negligible degree.

Eddy current loss on conductors caused by magnetic flux changing of rotor PM in the conductor section is another significant content to the overall stator winding losses of a high-speed PMBLDC motor [22]. Neglecting the axial end effect of the motor, dividing the stator into N layers in the radial direction, and assuming that the winding conductors are evenly distributed in each layer, the eddy current loss of conductors w_{we} can be calculated as follows [23]:

$$w_{we} = \frac{M}{128N}\pi D^4 \sigma l \omega_1^2 \sum_{j=1}^{N} \sum_{n=2k+1}^{\infty} n^2 \left(B_{rgjnm}^2 + B_{tgjnm}^2\right) \tag{3}$$

where M is the number of conductors, D is the diameter of the conductor, σ is the conductivity of conductor, l is the axial length of conductor, ω_1 is the angular frequency of the fundamental component, and B_{rgjnm} and B_{tgjnm} are the radial and tangential magnetic flux density amplitudes of the n-th harmonic at the j-layer conductors, $k = 0,1,2,3\ldots$.

It can be seen from the above-mentioned formula that the winding eddy current loss of slotted and slotless motor is directly related to the speed and internal magnetic field. Especially for the slotless motor, the winding is directly exposed to strong alternating magnetic field, so the winding eddy current loss is serious. This section focuses on the comparative study of the factors affecting the winding eddy current of slotted and slotless motors, including the number of parallel wires and the speed.

1) INFLUENCE OF MULTIPLE PARALLEL WIRES ON WINDING EDDY CURRENT LOSSES

Generally, winding eddy current loss can be effectively reduced by using multi-strand thin wound wires instead of single thick wire with the same total copper sectional area. However, the eddy current loss still exists in the thin conductor at high frequency. Figs. 9 and 10 show the eddy current density distributions of slotted and slotless motors at 60 krpm with different parallel numbers of wires. Compared Fig. 9 with Fig. 10, it can be found that: with the same size of wires, the maximum eddy current density in the winding of the slotted motor is much lower than that of the slotless motor. Moreover, the uniformity of eddy current distribution in the slotted motor is quite different from that of the slotless motor. As for slotted motor, due to the effect of slots, only magnetic flux leakage in slot produces certain eddy current in partial winding conductors, especially the conductors near the slot opening. However, the stator windings of slotless motors are directly exposed to alternating magnetic fields, so the eddy current distribution of different conductors is similar.

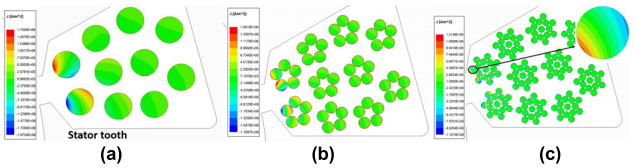

FIGURE 9. Eddy current distribution on conductors of slotted motor with different numbers of parallel wires: (a) 1 parallel wire, (b) 5 parallel wires, and (c) 15 parallel wires.

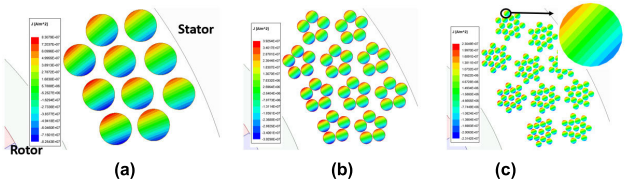

FIGURE 10. Eddy current distributions on conductors of slotless motors with different numbers of parallel wires: (a) 1 parallel wire, (b) 5 parallel wires, and (c) 15 parallel wires.

2) INFLUENCE OF DIFFERENT SPEEDS AND PARALLEL WIRE NUMBERS ON WINDING LOSSES

As mention above, the Joule loss of winding can be calculated as AC loss P_{ac}. The total winding losses (including Joule

losses and eddy current effect losses) of slotted and slotless high-speed PMBLDC motors with different speeds and parallel numbers are compared in Fig. 11.

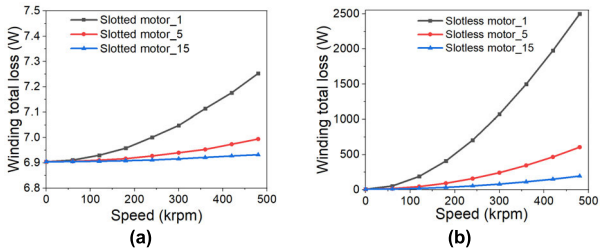

FIGURE 11. Total winding losses of slotted and slotless motors with different speeds and parallel numbers: (a) Slotted motor, and (b) Slotless motor.

It can be seen from Fig. 11 that: 1) with the increase of the speed, the total winding loss of the slotted motor increases, and the increasement is larger with lower parallel number. However, with the increase of speed, the total winding losses of slotless motor nonlinearly increase, and the increasement is also larger with less parallel number. 2) With the same number of parallel wires, the total winding losses of slotted motor is far less than that of slotless motor. This proves that the winding eddy current loss of slotless motor is much more sensitive to speed than that of the slotted motor.

The proportion of eddy current losses in total winding losses with different speeds and different parallel number of slotted and slotless motors is analyzed and shown in Fig.12. It can be found that: 1) the eddy current losses are greatly affected by the stator structure. For slotted motor, because the flux in slots is small, the winding eddy current loss accounts for no more than 3% of total winding losses. However, for slotless motor, because the winding is exposed to high frequency magnetic field directly, the winding eddy current loss plays a leading role in the total winding losses, and the proportion can reach about 98%. 2) The radio of winding eddy current loss increases with respect to the decrease of parallel number of wires. Combined with the above analysis of total winding losses, it is shown that the wire sectional area with 1 parallel number is too large and unsuitable for slotless high-speed PMBLDC motor in this paper. Therefore, 1 parallel wire is no longer studied.

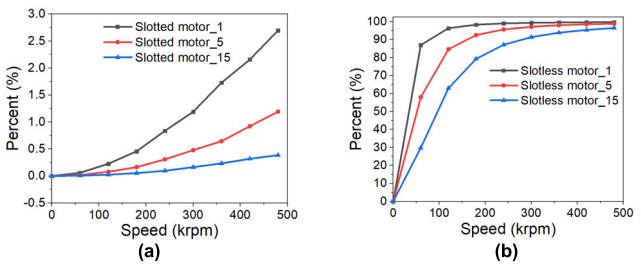

FIGURE 12. Ratio of winding eddy current losses to total winding losses: (a) slotted motor, and (b) slotless motor.

3) ROTOR LOSSES

When the PMBLDC motor runs at high speed, there exist iron loss of rotor back iron and eddy current loss in the PMs and retaining sleeve. The material of retaining sleeve is stainless steel, corresponding to a high conductivity. Due to the magnetic field shielding of rotor retaining sleeve, the iron loss of rotor back iron of slotted and slotless motors is very small. Thus, the rotor iron losses are not shown and neglected. The rotor losses only consider the eddy current losses in PMs and retaining sleeve caused by the harmonic components of magnetic field. The rotor eddy current loss is greatly affected by the rotating speed [24]. The rotor eddy current loss of slotted and slotless motor at no load varying with speed is shown in Fig. 13(a). It can be found that the rotor eddy current loss of slotted motor increases in a parabolic style. The rotor eddy current loss of slotless motor at no load is very small and can be neglected. Rotor eddy current losses of slotted and slotless motors at load varying with speed are shown in Fig. 13(b). It can be seen that the rotor eddy current loss at load of slotted motor is larger than that of slotless motor. Moreover, both of them increase nonlinearly as the increasing of speed.

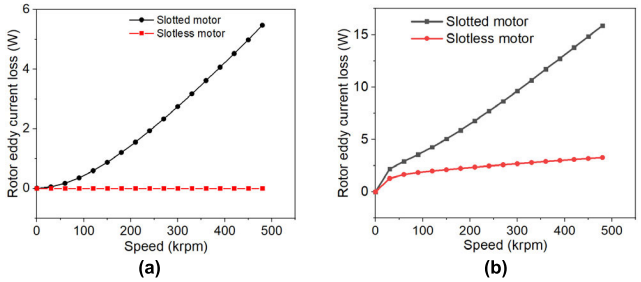

FIGURE 13. Rotor eddy current losses: (a) slotted and slotless motor at no load, and (b) slotted and slotless motors at load.

4) COMPARATIVE ANALYSIS OF TOTAL LOSSES

The losses versus speed with different materials of stator and rotor cores (35SW1900, 20SW1500) and different parallel numbers of wires (5, 15) of slotted and slotless motors at no load and load are compared in Figs. 14- 17, respectively. It can be seen that: 1) The rotor losses of both motors and winding loss of slotted motor are relatively small and have little influence on the total loss comparison. The total loss of slotted motor is dominated by the stator iron loss. As for slotless motor, the total loss is decided by both the winding loss and stator iron loss, and especially the winding loss plays the major role. 2) Comparing Fig. 14 and Fig. 16, when the parallel number of wires is 5, the wire diameter is relatively large (with 0.67 mm in this paper). Thus, the winding eddy current loss of slotless motor is much larger and plays a major role in the total losses. For slotted motor, the stator iron loss plays a major role. However, due to the large winding eddy current loss of slotless motor, the total loss of slotless motor is greater than that of slotted motor with 35SW1900 or 20SW1500. 3) Combining Fig. 14 and Fig. 15, with iron core

material of 35SW1900, when the parallel number of wires increases from 5 to 15, the wire diameter decreases much, so the winding eddy current loss of slotless motor decreases much. Moreover, the stator iron loss of 35SW1900 is larger and plays a bigger role, so the total loss of slotted motor is greater than that of slotless motor. 4) Comparing Fig. 15 and Fig. 17, when the parallel number of wires is 15, the wire diameter becomes much thinner (with 0.387 mm in this paper), the stator iron loss with 20SW1500 is much lower than that with 35SW1900. In the condition with 15 parallel strands of wires and 20SW1500, it is hard to give a simple conclusion whether slotted motor or slotless motor having lower total losses, which should be discussed separately. When the speed is in the range of about 0-300krpm under load condition, the total losses of slotless motor is smaller than that of slotted motor. When the speed is in the range of about 300krpm-480krpm under load condition, the total losses of slotless motor is greater than that of slotted motor. In general, the total load losses of slotted motor are closer to that of slotless motor in the full speed range. For no-load condition, when the speed is in the range of about 0-125krpm, the total losses of slotless motor is smaller than that of slotted motor; when the speed is in the range of about 125krpm - 480krpm, the total losses of slotless motor is greater than that of slotted motor.

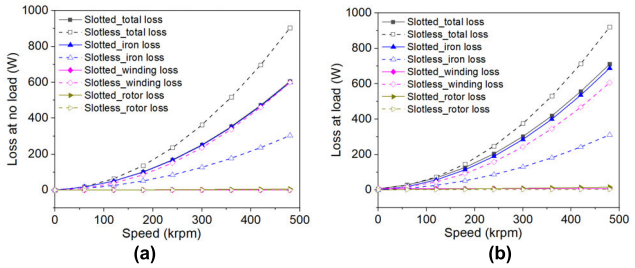

FIGURE 14. Losses of 35SW1900 with 5 parallel strands: (a) at no load, and (b) at load.

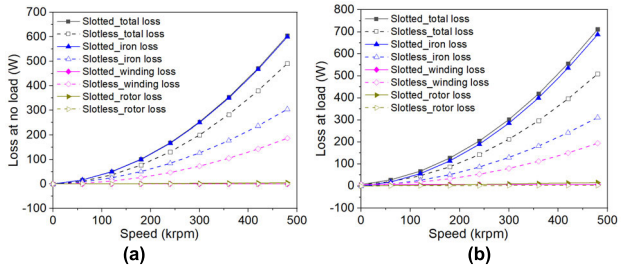

FIGURE 15. Losses of 35SW1900 with 15 parallel strands: (a) at no load, and (b) at load.

IV. THERMAL ANALYSIS

The losses in motors influence the thermal characteristics directly. High temperature may lead to irreversible demagnetization of PMs and winding short circuit and other faults, seriously affecting the reliability of the motors. Therefore,

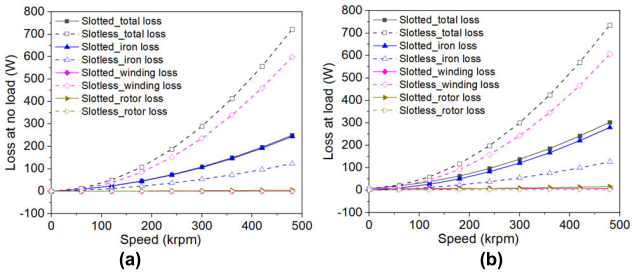

FIGURE 16. Losses of 20SW1500 with 5 parallel strands: (a) at no load, and (b) at load.

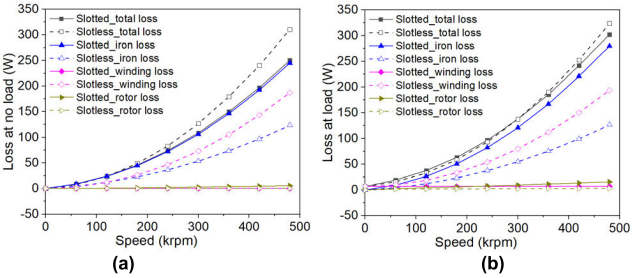

FIGURE 17. Losses of 20SW1500 with 15 parallel strands: (a) at no load, and (b) at load.

the thermal characteristics of slotted and slotless high-speed PMBLDC motors are researched based on the loss analysis above.

A. ESTABLISHMENT OF THERMAL ANALYSIS MODEL

In this paper, the characteristics of temperature rise of slotted and slotless motors in natural environment are studied. Heat conduction and convection are the main forms of heat dissipation, and thermal radiation is ignored here. For the motors studied in this paper, the winding distribution is complex and irregular. Thus, equivalent model of the stator winding for the slotted and slotless motors are established and shown in Fig. 18 [25]. Conductors in each actual or virtual slot are equivalent to a thermal conductor, and the insulating paint and air gap of all wires are equivalent to another thermal conductor wrapped around copper to form an equivalent insulating layer.

According to the thermal conductivity and thickness of the material, the equivalent thermal conductivity of the insulating material can be calculated according to [25]:

$$\lambda_{eq} = \sum_{i=1}^{n} \delta_i / \sum_{i=1}^{n} (\delta_i / \lambda_i) \tag{4}$$

where δ_i is the thickness of each insulating material (m), and λ_i is the thermal conductivity of each insulating material (W/m·K). The calculated equivalent thermal conductivity of the insulating layer of slotted motor and slotless motor are $\lambda_{eq1} = 0.043$ W/m·K and $\lambda_{eq2} = 0.042$ W/m·K, respectively. The other equivalent thermal conductivity parameters can also be calculated according to [25].

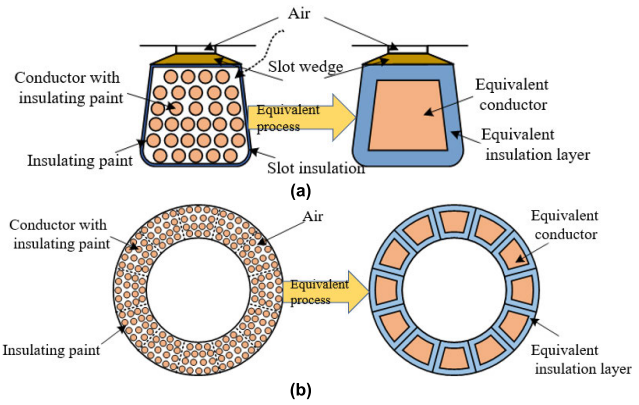

FIGURE 18. Equivalent thermal model of stator winding: (a) slotted motor, and (b) slotless motor.

TABLE 3. Thermal property of materials of motor main components.

Motor component	Material	Density (kg/m³)	Heat conductivity (W/m·K)	Specific heat (J/kg·K)
Motor shell	Aluminum alloy	2700	107	904
Iron core	20SW1500 35SW1900	7650	23.1 21	450
Stator winding	Copper	8933	400	385
Rotor retaining sleeve	Stainless steel	7750	15.1	480
PM	N38SH	7400	8.932	502.3

When calculating the thermal characteristics by ANSYS Workbench, the losses are the main heat source, including the stator iron loss, winding loss and rotor eddy current loss. The heat sources inside each part of the motor are assumed to be evenly distributed. The thermal properties of main component materials are shown in Table 3.

B. SIMULATION STUDY OF TEMPERATURE RISE

Slotted and slotless motors run continuously for 8000 s at speed of 60 krpm with natural cooling. Temperature rising curves of motors under no load and rated load with different silicon steel materials and different numbers of parallel wires are shown in Figs 19 and 20. The temperature of the slotted and slotless motors is basically stable after running for 40 min. In Fig. 21, motors with 20SW1500 are chosen to show the temperature distribution of different motor components under rated load condition. Moreover, the temperature distribution of PM is in the lower right corner of each figure.

It can be found that: 1) The winding temperature of slotless motor is always higher than that of slotted motor. Moreover, the winding temperature of slotless motor is the highest among temperature of different motor components of slotted and slotless motors. 2)The stator core temperature of slotted motor is higher than that of slotless motor in most cases except the case of no-load condition with 20SW1500 and

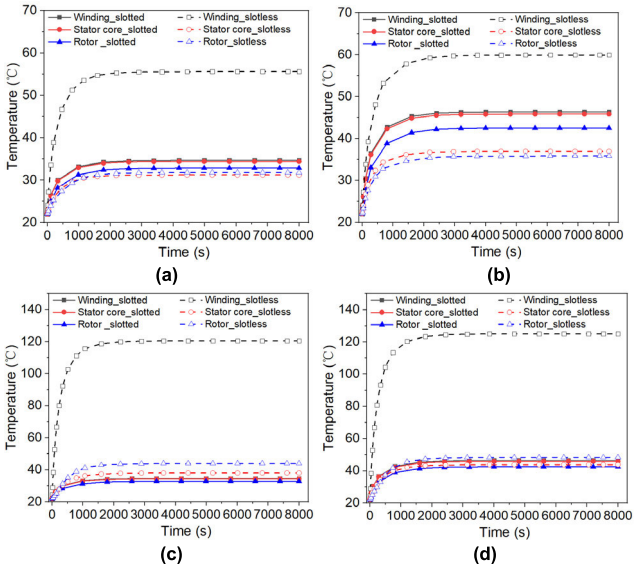

FIGURE 19. Temperature rising under no-load condition. (a) 20SW1500 with 15 parallel wires. (b) 35SW1900 motor with 15 parallel wires. (c) 20SW1500 with 5 parallel wires. (d) 35SW1900 with 5 parallel wires.

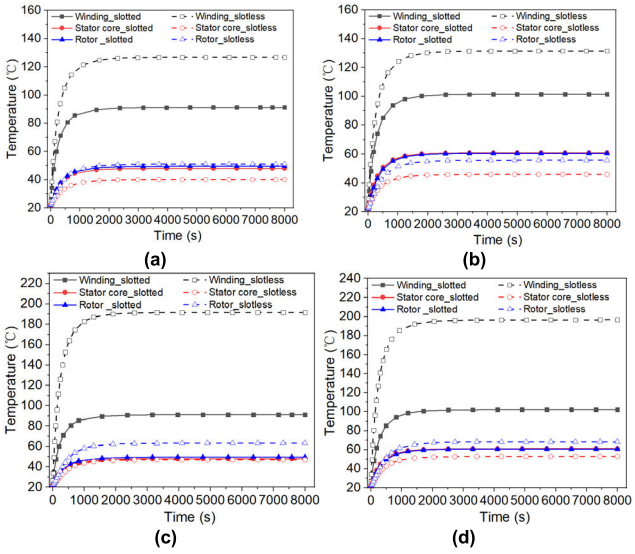

FIGURE 20. Temperature rising under rated load condition: (a) 20SW1500 with 15 parallel wires, (b) 35SW1900 motor with 15 parallel wires, (c) 20SW1500 with 5 parallel wires, and (d) 35SW1900 with 5 parallel wires.

5 parallel wires. It is due to that the winding eddy current loss plays a major role in the temperature rise of slotless motor at no load with 20SW1500 and 5 parallel wires. Therefore, the temperature of the stator core of slotless motor increases as a result of heat transfer. 3)The rotor temperatures for both slotted and slotless motors are relatively low. Comparing the rotor temperature and the losses, it can be found that the rotor temperature is basically positively related to motor total losses. 4) As for either slotted motor or slotless motor, the component temperature of motor with 35SW1900 is higher than corresponding component of motor with 20SW1500. 5)

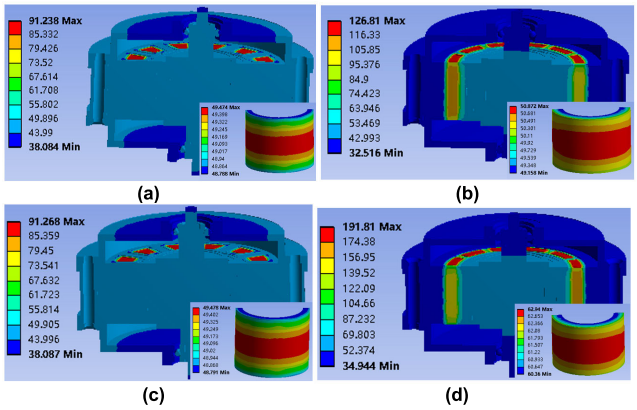

FIGURE 21. Steady state temperature distribution of slotted and slotless motors with 20SW1500 under rated load condition: (a) slotted motor with 15 parallel wires, (b) slotless motor with 15 parallel wires, (c) slotted motor with 5 parallel wires, and (d) slotless motor with 5 parallel wires.

On the whole, the temperature rise contrasts are consistent with the loss contrast of slotted and slotless motors.

V. PROTOTYPE EXPERIMENT

In order to verify the analysis results above, a 2-pole 12-slot high-speed PMBLDC slotted motor prototype is manufactured and the test platform is established, as shown in Fig. 22.

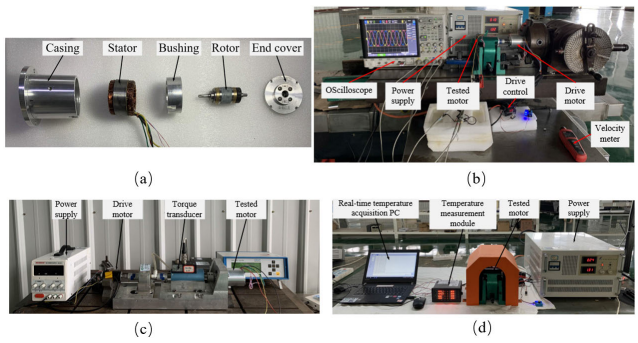

FIGURE 22. Prototype and test platform: (a) prototype, (b) back EMF test platform, (c) iron loss test platform, and (d) temperature rise test platform.

The no-load back EMF at 6 krpm of the prototype is measured by the motor drag test method. Since the no-load back EMF is proportional to the speed, the no-load back EMF at 60 krpm can be inferred. The simulated and test no-load back EMFs are compared in Fig. 23, and it can be seen that they are in good agreement. The peak-to-peak values of no-load back EMF of A phase, B phase and C phase windings calculated by simulation are slightly higher than the measured values by 1.3%, 0.9% and 0.9%, respectively.

In order to verify the accuracy of losses calculation results, no-load iron loss and winding eddy current loss of the slotted motor prototype at rotational speed n_k =0∼6krpm (n_k >0) are tested, which is limited by the installation accuracy of the test platform.

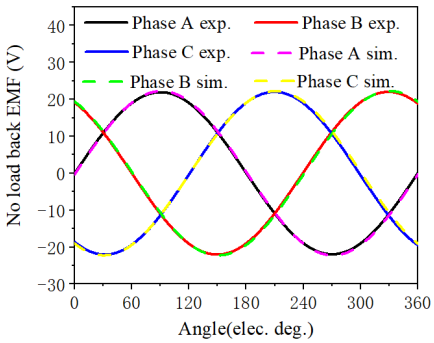

FIGURE 23. No-load back EMF test waveform and simulation waveform.

In the process of experimental tested of losses, the principle of controlling a single variable is adopted to replace the corresponding stator/rotor parts for repeated testing. First of all, the stator without winding is assembled with the rotor without PMs, and the input power at different speeds is tested, which is mechanical loss p_{mech}. Secondly, the stator is kept unchanged, and the PMs are installed on the rotor to test the input power at different speeds, which mainly includes p_{mech} and stator iron loss p_{sFe} (the eddy current loss of permanent magnet and rotor back iron can be ignored). Comparing the losses in the two tests, the stator iron loss can be obtained. Finally, keeping the rotor unchanged, the winding is installed to test the input power at different speeds, which includes the p_{mech} and stator iron loss p_{sFe} and winding eddy current loss p_{weddy}, then the winding eddy current loss can be obtained easily. The measured values and simulation results of iron losses are shown in Fig. 24(a). It can be seen that the iron loss increases with the increase of the speed, and the change trend is consistent with the simulation results. The tested eddy current loss of the winding is zero, which accords with the simulation results.

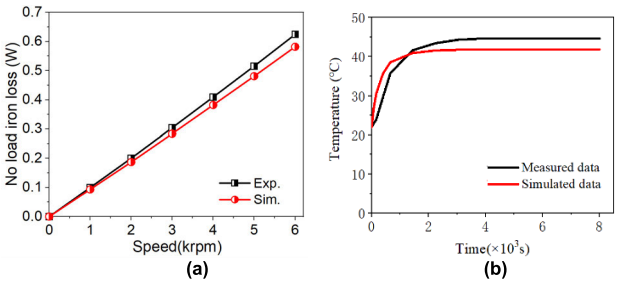

FIGURE 24. Comparison between simulation and measured results: (a) no-load iron losses, and (b) no-load dynamic temperature rise.

In order to verify the accuracy of the calculated results of the motor temperature field, the no-load temperature rise is tested using A PT100 temperature sensor placed at the motor slot opening. In the natural environment, the prototype rotates at the rated speed of 60 krpm, and the upper computer collects the measured temperature in real time. Fig. 24(b) shows the measured and simulated temperature rise curves of the motor running at rated speed (60 krpm) for about two hours without

load. It is shown that the temperature of the prototype is basically stable after no-load operation for about 50 min. The measured steady-state temperature is 44.6°, which is 2.6° higher than the simulated result, which is basically consistent with each other and verifies the correctness of the thermal analysis model and simulation method.

VI. CONCLUSION

The electromagnetic performances, electromagnetic losses and thermal characteristics of slotted and slotless high-speed PMBLDC motors are comprehensively compared in this paper.

(1) The electromagnetic performances of slotless and slotted motors are compared. Due to the elimination of the slot structure, the slotless motor has more uniform magnetic density distribution, lower harmonic content, better overload capability, lower torque fluctuation and zero cogging torque. However, the slotted motor uses small amounts of PMs, i.e., with a higher PM utilization rate.

(2) The stator iron core losses, winding losses, rotor losses and total electromagnetic losses of slotted and slotless motors are discussed and compared considering the influences of silicon steel materials, parallel wires and rotating speed, respectively.

(3) Based on the losses calculation results, the temperature rise characteristics of slotted and slotless motors with different silicon steel materials and number of parallel wires are studied. The maximum temperature is located in the stator winding of slotted and slotless motors. Moreover, the temperature comparison corresponds to the loss comparison of slotted and slotless motor.

(4) After comprehensive comparison within the full range of 0-480krpm, it is can be concluded that when the focus is on reducing the maximum temperature of the motor and improving the utilization rate of PMs, or acquiring smaller winding losses and temperature, it is preferred to choose a slotted motor. Thinner wire diameter is necessary for slotless machine to reduce total losses. When thinner wires are adopted, the total loss of slotless motor is lower or close to that of slotted motor. In addition to considering the no-load, load and over load electromagnetic performances, the slotless motor with thinner wires is more preferred.

(5) At last, a prototype of a high-speed PMBLDC motor is manufactured and tested, and the experiment results validate the FEM simulations.

REFERENCES

[1] T. R. He, Z. Q. Zhu, F. Xu, H. Bin, D. Wu, L. M. Gong, and J. T. Chen, "Comparative study of 6-slot/2-pole high-speed permanent magnet motors with different winding configurations," *IEEE Trans. Ind. Appl.*, vol. 57, no. 6, pp. 5864–5875, Nov. 2021.

[2] G. Liu, M. Liu, Y. Zhang, H. Wang, and C. Gerada, "High-speed permanent magnet synchronous motor iron loss calculation method considering multiphysics factors," *IEEE Trans. Ind. Electron.*, vol. 67, no. 7, pp. 5360–5368, Jul. 2020.

[3] E. Kurvinen, C. Di, I. Petrov, J. Nerg, O. Liukkonen, R. P. Jastrzebski, D. Kepsu, P. Jaatinen, L. Aarniovuori, E. Sikanen, J. Pyrhönen, J. Sopanen, O. Pyrhönen, M. Niemelä, and T. Kangasmäki, "Design and manufacturing of a modular low-voltage multimegawatt high-speed solid-rotor induction motor," *IEEE Trans. Ind. Appl.*, vol. 57, no. 6, pp. 6903–6912, Nov. 2021.

[4] L. Yang, Z. Q. Zhu, H. Bin, Z. Zhang, and L. Gong, "Virtual third harmonic back EMF-based sensorless drive for high-speed BLDC motors considering machine parameter asymmetries," *IEEE Trans. Ind. Appl.*, vol. 57, no. 1, pp. 306–315, Jan. 2021.

[5] Y. Tang, Y. He, F. Wang, and R. Kennel, "Voltage-sourced converter fed high-speed switched reluctance motor drive system with energy feedback and near-unity power factor," *IEEE Trans. Ind. Electron.*, vol. 69, no. 4, pp. 3460–3470, Apr. 2022.

[6] B. Dong, K. Wang, B. Han, and S. Zheng, "Thermal analysis and experimental validation of a 30 kW 60000 r/min high-speed permanent magnet motor with magnetic bearings," *IEEE Access*, vol. 7, pp. 92184–92192, 2019.

[7] M. S. Islam, R. Mikail, and I. Husain, "Field weakening operation of slotless permanent magnet machines using stator embedded inductor," *IEEE Trans. Ind. Appl.*, vol. 57, no. 3, pp. 2387–2397, May 2021.

[8] C. Zhang, L. Chen, X. Wang, and R. Tang, "Loss calculation and thermal analysis for high-speed permanent magnet synchronous machines," *IEEE Access*, vol. 8, pp. 92627–92636, 2020.

[9] K. G. Il, H. Man Seung, Y. S. Hak, and L. Y. Cheol, "The study on BLDC motor compressor using SMC," in *Proc. IEEE 6th Int. Power Electron. Motion Control Conf.*, May 2009, pp. 1930–1933.

[10] G. Du, W. Xu, J. Zhu, and N. Huang, "Power loss and thermal analysis for high-power high-speed permanent magnet machines," *IEEE Trans. Ind. Electron.*, vol. 67, no. 4, pp. 2722–2733, Apr. 2020.

[11] A. Tüysüz, T. Achtnich, C. Zwyssig, and J. W. Kolar, "A 300 000-r/min magnetically levitated reaction wheel demonstrator," *IEEE Trans. Ind. Electron.*, vol. 66, no. 8, pp. 6404–6407, Aug. 2019.

[12] P. Puentener, M. Schuck, D. Steinert, T. Nussbaumer, and J. W. Kolar, "A 150 000-r/min bearingless slice motor," *IEEE/ASME Trans. Mechatronics*, vol. 23, no. 6, pp. 2963–2967, Dec. 2018.

[13] M. Markovic and Y. Perriard, "Analytical solution for rotor eddy-current losses in a slotless permanent-magnet motor: The case of current sheet excitation," *IEEE Trans. Magn.*, vol. 44, no. 3, pp. 386–393, Mar. 2008.

[14] M. M. Radulescu, V. Iancu, K. Biro, and H. Hedesiu, "Design and control considerations for slotless electronically-commutated permanent-magnet servomotors," in *Proc. Medit. Electrotech. Conf.*, Apr. 1991, pp. 131–135.

[15] A. Mujianto, M. Nizam, and Inayati, "Comparation of the slotless brushless DC motor (BLDC) and slotted BLDC using 2D modeling," in *Proc. Int. Conf. Electr. Eng. Comput. Sci. (ICEECS)*, Nov. 2014, pp. 212–214.

[16] W. Cheng, G. Cao, Z. Deng, L. Xiao, and M. Li, "Torque comparison between slotless and slotted ultra-high-speed AFPM motors using analytical method," *IEEE Trans. Magn.*, vol. 58, no. 2, pp. 1–5, Feb. 2022.

[17] N. Dave, G. Vakil, Z. Xu, C. Gerada, H. Zhang, and D. Gerada, "Comparison of slotted and slotless PM machines for high kW/kg aerospace applications," in *Proc. 23rd Int. Conf. Electr. Mach. Syst. (ICEMS)*, Nov. 2020, pp. 609–613.

[18] N. Verbeek, F. Baudart, and B. Dehez, "Preliminary comparison of slotless FPC winding and slotted wire winding PM machines," in *Proc. 23rd Int. Conf. Electr. Mach. Syst. (ICEMS)*, Nov. 2020, pp. 1892–1897.

[19] F. Xu, T. R. He, Z. Q. Zhu, H. Bin, D. Wu, L. M. Gong, and J. T. Chen, "Comparison of slotted and slotless high-speed permanent magnet motors with toroidal windings," in *Proc. IEEE Energy Convers. Congr. Expo. (ECCE)*, Oct. 2022, pp. 1–8.

[20] J. Zhao, W. Fu, X. Liu, L. Yang, and L. Yang, "Research on performances of slotted/slotless high-speed PM BLDC motors with different PM magnetizations," in *Proc. IEEE 4th Int. Electr. Energy Conf. (CIEEC)*, May 2021, pp. 1–6.

[21] P. N. Murgatroyd, "Calculation of proximity losses in multistranded conductor bunches," *IEE Proc. A, Phys. Sci., Meas. Instrum., Manage. Educ.*, vol. 136, no. 3, pp. 115–120, May 1989.

[22] Q. Gao, X. Wang, Z. Deng, and Y. Zhang, "Loss calculation, analysis, and separation method of 550 000 r/min ultrahigh-speed permanent magnet motor," *IEEE Trans. Ind. Electron.*, vol. 70, no. 4, pp. 3471–3481, Apr. 2023.

[23] P. H. Tang, Y. M. Qi, G. H. Huang, and T. C. Li, "Eddy current loss analysis of ironless flywheel electric machine's winding," *Trans. China Electro. Soc.*, vol. 25, no. 3, pp. 27–32, Mar. 2010.

[24] J. Wang, K. Atallah, R. Chin, W. M. Arshad, and H. Lendenmann, "Rotor eddy-current loss in permanent-magnet brushless AC machines," *IEEE Trans. Magn.*, vol. 46, no. 7, pp. 2701–2707, Jul. 2010.
[25] J. Bai, Y. Liu, Y. Sui, C. Tong, Q. Zhao, and J. Zhang, "Investigation of the cooling and thermal-measuring system of a compound-structure permanent-magnet synchronous machine," *Energies*, vol. 7, no. 3, pp. 1393–1426, Mar. 2014.

JING ZHAO (Member, IEEE) received the B.Sc. degree in electrical engineering from the Hebei University of Technology, Tianjin, China, in 2005, and the M.Sc. and Ph.D. degrees in electrical engineering from the Harbin Institute of Technology, Harbin, China, in 2007 and 2011, respectively.

She is currently an Associate Professor with the School of Automation, Beijing Institute of Technology, Beijing, China. Her research interests include electric machines and drive systems used for renewable energy and special servo machine systems.

WEI HE was born in Zhuozhou, China. He received the B.Sc. and M.Sc. degrees in electrical engineering from the Hebei University of Science and Technology, Shijiazhuang, China, in 2016 and 2019, respectively. He is currently pursuing the Ph.D. degree in control science and engineering with the Beijing Institute of Technology, Beijing, China.

His research interests include high-speed permanent magnet motors and spherical motors.

WENQI FU received the B.Sc. degree in automation from the North China University of Technology, Beijing, China, in 2018, and the M.Sc. degree from the Beijing Institute of Technology, Beijing, in 2021.

She is currently with the Beijing Institute of Aerospace Control Devices, Beijing. Her research interests include modeling and design of PM machines and new permanent magnet motor systems.

YU DING received the B.Sc. and M.Sc. degrees from Qufu Normal University, Rizhao, China, in 2017 and 2020, respectively. She is currently pursuing the Ph.D. degree with the School of Automation, Beijing Institute of Technology, Beijing, China.

Her current research interest includes the coreless permanent magnet brushless motor.

YOUGUANG GUO (Senior Member, IEEE) received the B.E. degree in electrical engineering from the Huazhong University of Science and Technology, Wuhan, China, in 1985, the M.E. degree in electrical engineering from Zhejiang University, Hangzhou, China, in 1988, and the Ph.D. degree in electrical engineering from the University of Technology Sydney (UTS), Ultimo, Australia, in 2004. He is currently an Associate Professor with School of Electrical and Data Engineering, UTS. His research interests include measurement and characterization of magnetic properties of magnetic materials, numerical analysis of electromagnetic fields, electrical machine design and optimization, power electronic drives, and motor control.